Stress measurements in the main cable of a suspension bridge under dead and traffic loads

M. Talbot & J.F. Laflamme
Ministère des Transports du Québec, Québec, Canada

B. Glišić
Smartec SA, Lugano Switzerland

ABSTRACT: The realistic evaluation of the safety factors of a main cable relies on two different steps. The first step entails the determination of the actual physical state of the cable, in order to get a resistance value. This is why the main cable of the Île-d'Orléans bridge was opened at a few specific cross-section locations during the summer of 2006. This access also enabled the *in-situ* measurements of the actual total dead and live loading of the cable strands, which is the second step of the evaluation. Dead load has been obtained experimentally using laser vibrometry, and compared to theory. For dynamic loads, load tests of the opened cable were carried out. Six SOFO sensors were used in order to obtain a representative distribution of the live load in the strands of the main cable from top to bottom of the cross-section of the cable caused by two weighted trucks. The resulting stress gradients in the strands are presented, along with their dynamic amplification factors.

1 INTRODUCTION

Describing the dynamic behaviour of large cable bridges is actually a very frequent and relevant application in the field of experimental vibration analysis for civil engineering structures. This interest is due to the fact that these bridges are usually very strategic structures, and are known to be very sensitive to vibrations. The global 3D dynamic behaviour of these bridges and local hanger or stay cable vibrations has been studied extensively in the literature over the past few years. However, few studies have described the specific aspects of the strand dynamic deformation in the main parabolic cables to date.

In the particular case of the Île-d'Orléans bridge near Québec city, Canada, there are similarities with the Lions' Gate Bridge in Vancouver, Canada. The Île-d'Orléans bridge was opened to traffic in 1935, which is more than 72 years ago (Fig 1).

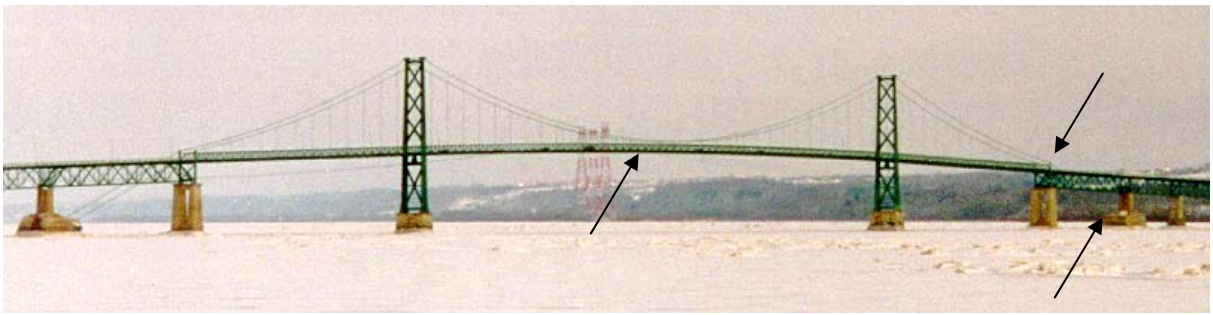

Figure 1. Side view of the Île-d'Orléans bridge (arrows point to locations where the main cable was opened and the anchor block was tested).

It measures 722 m between anchor blocks, and has three spans of 127 m, 323 m (centre span), and 127 m in length respectively. The bridge has been subjected to different measurements campaign in order to evaluate its condition and various aspects of its structural behaviour by Talbot (2001, 2002); Talbot & Stoyanoff (2005); Pridham et al. (2006); and Talbot & Laflamme (2007).

2 OPENING THE MAIN CABLE

In order to evaluate a suspension bridge, it is necessary to make a series of specific openings in the main cable, which is the most important element of a suspended structure, in order to expose the wires so that the requisite measurements can be made. Unlike stay-cables or hangers, the main cable is usually hidden from view by a protective covering. The recently published guide on the inspection of such cables (NCHRP 534, 2004) was used as a basis for defining the steps to be followed. However, the guide had to be adapted in light of the fact that the cable of the Île-d'Orléans bridge cable is not made up of thousands of parallel wires, but rather of 37 twisted strands (Fig 2).

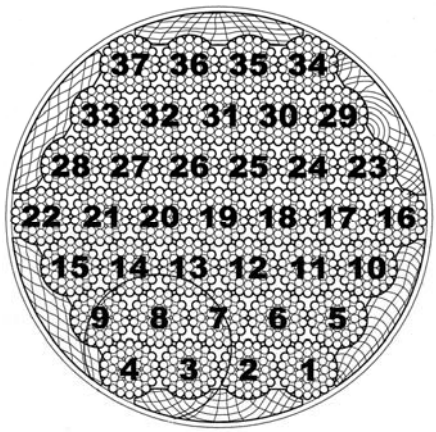

Figure 2. Typical cable section (37 strands, 1591 wires in total).

A number of authors have discussed the various aspects that must be considered when assessing the condition of cables and strands. In addition to the concrete examples that are given in Stahl & Gagnon (1996), there are the relevant experimental and theoretical analyses in Brevet et al. (2004a, b). The aspects relating to the calculation of the strength and state of the main cable have been fully described by Elachachi et al. (2005), Crémona (2003), and Mahmoud (2006). The importance of a detailed inspection and *in-situ* measurements of the main cable was clearly demonstrated by Kretz et al. (2006) and Godart et al. (2001) in the case of the Aquitaine bridge, where the discovery of a severely corroded cable with dozens of broken wires ultimately led to the complete replacement of the suspension cable.

A total of six openings were made in 2006, with the intention of being as exhaustive as possible, in particular by measuring the thickness of the galvanized layer at hundreds of points using an Elcometer, and a boroscope camera to take images of the inside of the cable, and extracting several metres of wires at each of the six openings for analysis and lab testing (dissolution and other zinc-thickness tests, as well as proof-load tests). The overall finding that emerged from these tests is that, given its age, the main cable was in remarkably good condition compared to similar structures elsewhere in the world. No broken wires were found. Brown corrosion (iron oxide) caused by the complete disappearance of the galvanized layer was limited to small, isolated areas. However, a fine layer of white corrosion (zinc oxide) was observed on much of the external surface of the wires of the 18 external strands.

According to our measurements, the thickness of the layer of zinc ranged from 44 μm to 65 μm (for a theoretical value of approximately 50 μm), which is excellent. The elastic strength (840 MPa to 886 MPa) and breaking strength (1543 MPa to 1650 MPa) are also close to those of

the wires when they were new at the time of construction (Talbot & Laflamme, 2007). Based on the strength of these clear results, we were able to reliably and precisely quantify the structural state of the main cable, and to maintain the cable's strength at its estimated pre-opening value.

3 MEASUREMENT OF STRAND STRESS UNDER DEAD LOAD

Using a variant of the vibrating string theory, we were able to determine the stresses in the strands of the main cable of the Île-d'Orléans bridge. The same approach has previously been cited by several authors in connection with cables, hangers, cable stays, and strands in general. A detailed description of the theory and the technical considerations can be found in the reports of several authors, including Cunha & Caetano (1999), Gourmelon (1986, 1997), Robert (1993), Siegert et al. (2005), and Gautier et al. (2005), and in applications such as Talbot (2001). These investigations demonstrate that pure vibrating string theory, without flexional rigidity, is not valid for strand lengths of several metres, as was the case with the main cable. Therefore, it is important to correctly define the rigidity and the boundary conditions at the extremities, as well as the true effective length of the vibrating system.

The vibrometer that we used was the Polytec PDV-100, which measures speed by laser interferometry. We then applied an FFT algorithm in order to obtain the vibration frequencies. The data was acquired for 65 second, with a sampling frequency of 2,000 Hz. Precautions were taken in order to ensure a high-quality signal and to prevent noise contamination (from the passing trucks). The measurements were usually taken when no vehicles were present on the centre section of the deck, and were repeated several times in order to obtain valid mean frequencies. In order to allow the strand to vibrate freely in relation to the main cable as a whole, the strand was raised from the cable by inserting hardwood wedges at the ends of the hangers, as shown in Figure 3. The wedges were inserted near the hangers, in order to achieve the greatest free vibration length possible (i.e.: 7.37 m). A strip of reflective tape was attached to the strand so that the laser signal would be accurately reflected. The position of the point of measurement was calculated in order to maintain amplitude at all times, and therefore, to prevent knotting. The strand was excited by a low-impact blow of the naked hand. This was the method used to test the 18 strands that form the circumference of the main cable, as well as the 37 strands in the four anchorage chambers.

Figure 3. Laser vibrometry tests.

The typical results for a strand (#22 at the centre-west opening) are shown in Table 1. The theoretical values are taken from a non-linear finite element model, which accounts for the flexional rigidity of the strand section, and the most realistic boundary conditions were those of clamped ends. The theoretical pure vibrating string values are also given for comparison purposes. Table 2 shows the stresses that were obtained for two of the opened segments, and sum-

marizes the results for the four anchorage chambers. On average, the observed values are close to the values of the finite element model (265, 260, and 284 kN, respectively). However, there are some differences within a given section. There is a slight gradient, which is not very significant (the precision of the method is on the order of 5%) for the opened sections, but much more significant for the anchorage chambers (i.e.: approximately 50 kN from top to bottom).

Table 1. Typical frequency values for strand #22 at the centre-west cable opening.

Mode	Frequency 3D model (Hz)	Frequency experimental values (Hz)	Ratio of experimental frequencies fi / f1	Difference experimental 3D model (%)	Frequency string model (Hz)	Ratio of string frequencies fi / f1	Difference experimental string model (%)
1	14.74	14.74	1.00	0.00	14.31	1.00	-2.92
2	29.75	29.82	2.02	-0.23	28.62	2.00	-4.02
3	45.29	45.41	3.08	-0.26	42.93	3.00	-5.46
4	61.61	61.50	4.17	0.18	57.24	4.00	-6.93
5	78.90	78.55	5.33	0.45	71.55	5.00	-8.91
6	97.36	97.09	6.59	0.28	85.86	6.00	-11.57
7	117.13	116.64	7.91	0.42	100.17	7.00	-14.12
8	138.35	137.54	9.33	0.59	114.48	8.00	-16.77
9	161.10	158.95	10.78	1.35	128.79	9.00	-18.97

Table 2. Summary of the dead load stress values in the strands at three typical locations.

Table 2a. South-West opening

		270	275	265	286		274
	261	*	*	*	*	310	286
	262	*	*	*	*	263	263
Mean value for the 18 strands:	270	*	*	*	*	270	270
271kN	261	*	*	*	*	262	262
	269	*	*	*	*	275	272
*: Could not be measured		263	262	270	278		268
Mean value per column:	265	267	269	268	282	276	

Mean value per row :

Table 2b. Centre West opening

		274	270	266	273		271
	267	*	*	*	*	267	267
	265	*	*	*	*	270	267
Mean value for the 18 strands:	268	*	*	*	*	271	269
266 kN	263	*	*	*	*	265	264
	268	*	*	*	*	266	267
*: Could not be measured		262	262	253	263		260
Mean value per column:	266	268	266	260	268	268	

Mean value per row :

Table 2c. Mean value for the 4 anchorage chambers

		266	273	276	267		270
	275	286	293	282	285	286	284
	284	280	269	263	283	292	279
Mean value for the 148 (4x37) strands:	303	285	265	269	290	311	287
291 kN	300	282	291	283	285	308	291
	315	306	303	303	302	321	308
		330	310	315	329		321
Mean value per column:	295	291	286	284	292	304	

Mean value per row :

4 MEASUREMENT OF STRAND STRESS UNDER TRAFFIC LOADS

In order to measure the stresses induced in the strands by traffic loads, the deformations of certain strands of the centre-east section of the main cable (Fig 4) and in the south anchorage chamber (Fig 5) were measured under controlled traffic conditions, using two 12-wheel trucks, each having a scale weight of slightly more than 30,000 kg. Quasi-static responses (at 7 km/h) and dynamic responses (at 72 km/h – the maximum safe speed for two trucks) were tested. The tests reported on here were carried out during the day, at a time when the bridge was completely closed to normal traffic so that the test vehicles could travel side by side from south to north in the two narrow driving lanes.

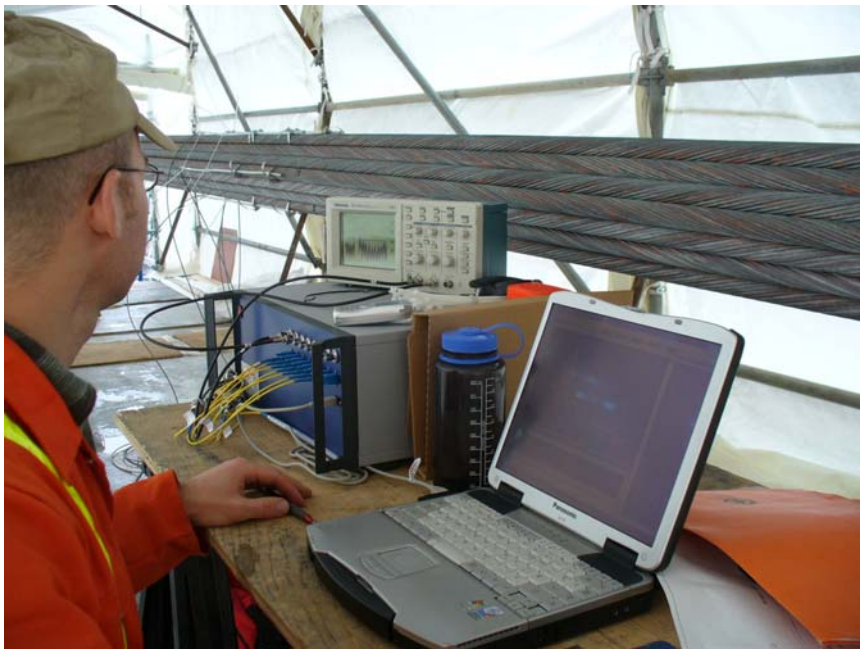

Figure 4. SOFO sensors, open cable section.

Figure 5. SOFO sensors, cable section in the anchorage chamber.

The Dynamic SOFO system and the SMARTEC SOFO deformation sensors were used for this project. The sensors are classified as “long base” sensors, because they can be manufactured with base lengths from 20 cm up to several metres. In this project, we used sensors with a base length of 30 cm. The sensors are protected by a plastic casing. The active part of the sensor is located between two steel mechanical clamp points on the strands, and consists of two optical fibres: an “active fibre” that is fixed between the two attach points; and a “reference fibre”, which is left free between the clamp points, that measures the effects of temperature. Relative movements of the two extremities of the base cause the change of difference in length between the two fibers. The light is passed in the Michelson interferometer, composed of two fibers in the SOFO sensors, and is reflected back to the demodulation system. A Mach-Zehnder interferometer with an active phase modulator is used as demodulation interferometer, which retrieves the change of difference in length between the active and reference fiber (Del Grosso et al., 2005). The sampling frequency was 250 Hz for the quasi-static response measurements, and 500 Hz for the dynamic response measurements. Six SOFO sensors were placed (Figs 4-5) at the corners of a hexagon formed by the main cable, as shown in Figures 6 to 9.

The redundancy provided by six sensors was ultimately quite useful, because some of the sensors did not function properly at all times. Having five functioning sensors meant that we were always able to calculate the resulting stresses. In fact, a minimum of four sensors is required in order to measure the four internal forces (axial, two moments, and one bi-moment), as is the case with measurements on steel sections (Talbot et al., 1993). This approach yields an approximation, because it assumes that the section that is made up of 37 strands behaves as a perfectly cohesive whole, which is probably not always the case. Still, it can highlight if the cable does not behave simply like a purely axial element, which conventional suspension bridge theory states that it should.

Figures 6 to 9 present selected findings for a complete vehicle run, and Tables 3 and 4 summarize the significant values and calculations. There is a notable difference in the deformations recorded by the six sensors, which suggests that the main cable does not behave as a purely axial element. Table 3 shows in particular the ratios for the anchorage chamber, which are approximately twice as high. These considerable differences are all the more important in light of the fact that the mean stress in the anchorage chambers is greater than at the centre of the bridge, because the angle of the cable is greater, in accordance with suspension bridge theory.

The resulting axial (strand mean) stresses were calculated, and they compare favourably with the theoretical values yielded by the 3D finite element model. The maximal theoretical stress for the centre was 466.6 kN, while the experimentally observed stress was 429.0 kN. The theoretical stress for the anchorage chamber was 495.3 kN, compared to the experimentally observed stress of 438.6 kN (the model was originally calibrated to be slightly conservative). The sensor values and the calculation of a main moment (not shown here) are indicative of the stress gradient. At the centre of the bridge, the base of the cable tends to be overstressed, whereas the opposite is true for the anchorage chamber.

Table 4 summarizes the dynamic amplification values for each sensor. The mean ratio is approximately 1.15. This value is useful, because no analytical values were available in the literature for the dynamic amplification of stresses in the main cables of suspension bridges in general.

The dynamic behaviour that is depicted in Figures 8 and 9 was also analyzed for its frequency content. The behaviour of the freely vibrating part of the cable at the centre was dominated by the bridge’s overall higher bending mode (dominant frequency of 0.58 Hz). In the anchorage chamber, two distinct groups of frequencies were observed. The frequencies of one group correspond to the free vibration of separate (vibrating string-type) strands, with high values of 83.4, 168.6, and 250.0 Hz (3rd, 6th, and 8th modes). The other group of very low frequencies (0.012, 0.06, …, 0.22 Hz) is the result of beat frequency phenomena between adjacent vibrating wires.

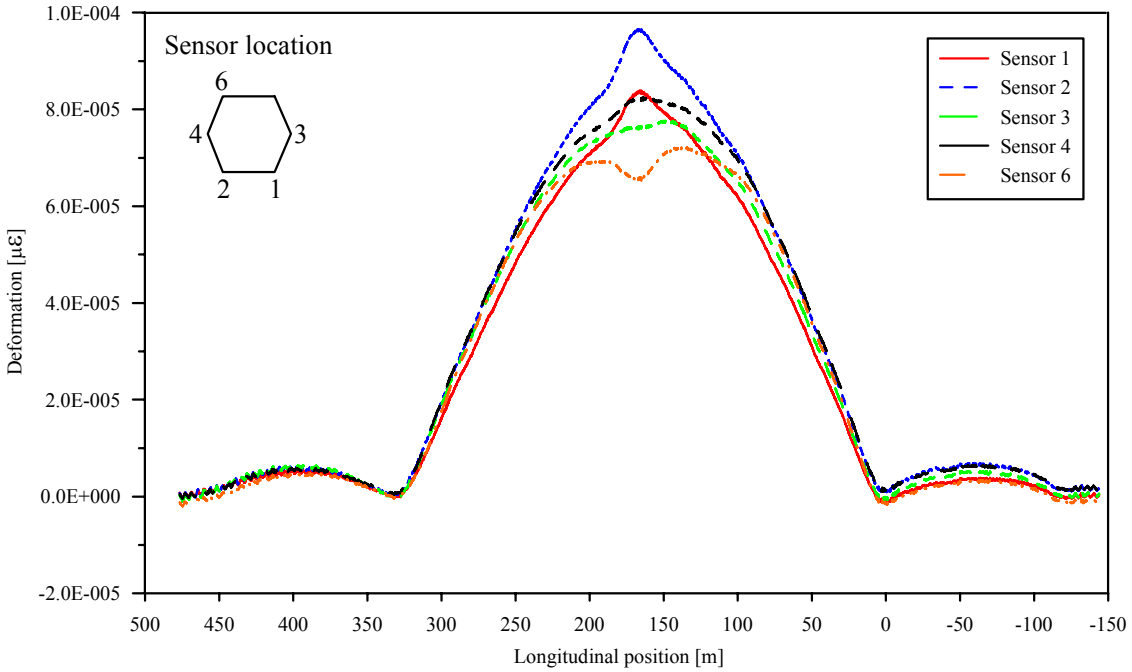

Figure 6. SOFO deformation sensor readings at the centre of the bridge for 2 trucks moving at 7 km/h.

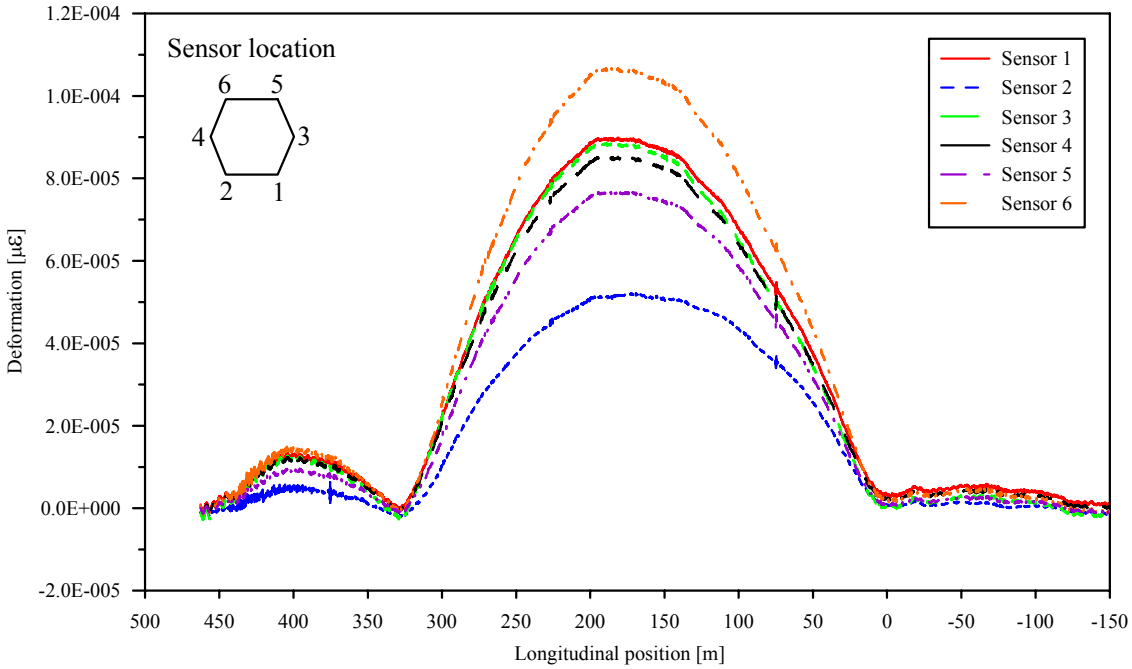

Figure 7. SOFO deformation sensor readings at the anchor block for 2 trucks moving at 7 km/h.

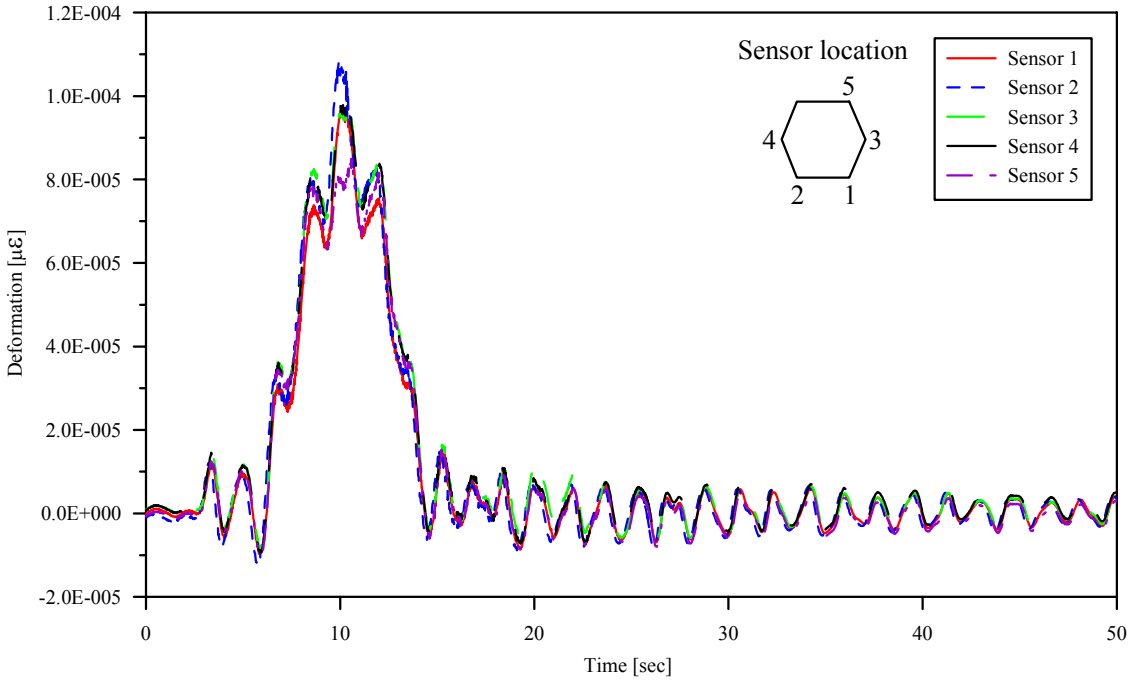

Figure 8. SOFO deformation sensor readings at the centre of the bridge for 2 trucks moving at 72 km/h.

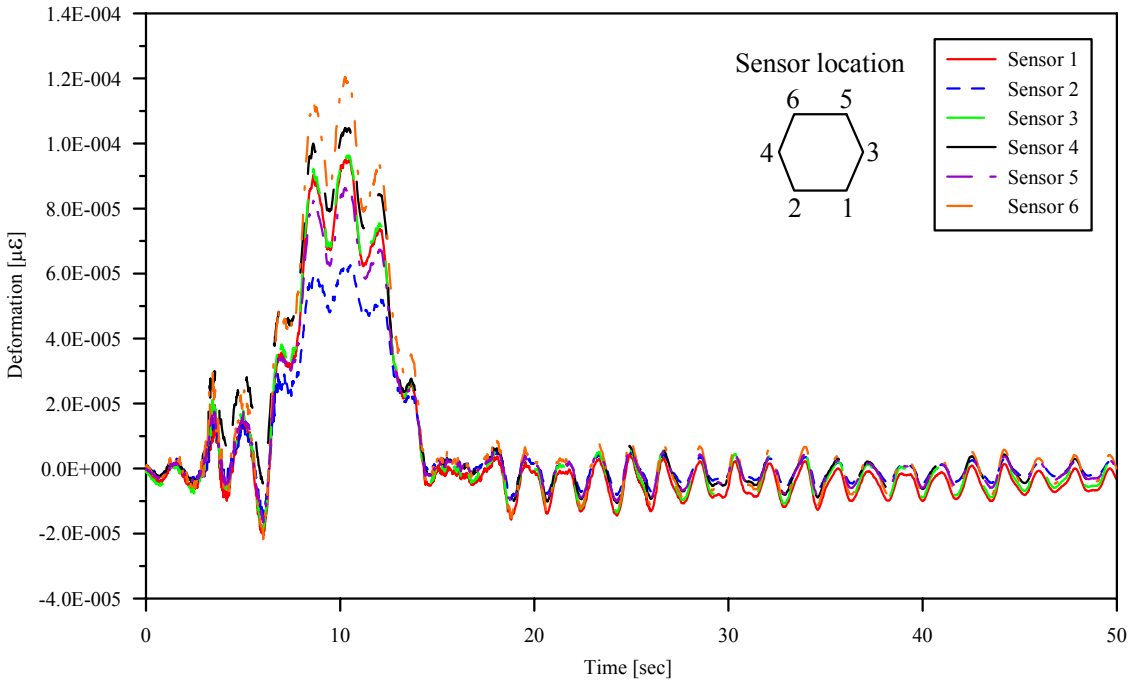

Figure 9. SOFO deformation sensor readings at the anchor block for 2 trucks moving at 72 km/h.

Table 3. Summary of the stress gradients in the strands at two typical locations.

Test setup	Simultaneous values of the sensors						Ratio of maximum value to minimum value of sensors
	Sensor 1 (MPa)	Sensor 2 (MPa)	Sensor 3 (MPa)	Sensor 4 (MPa)	Sensor 5 (MPa)	Sensor 6 (MPa)	
Centre-east at 7 km/h	16.78	19.36	15.28	16.48	*	13.20	1.47
Centre-east at 72 km/h	19.29	21.24	19.19	19.49	15.97	*	1.33
Anchorage at 7 km/h	17.98	10.35	17.71	17.05	15.36	21.34	2.06
Anchorage at 72 km/h	19.00	12.15	19.30	20.96	17.26	24.07	1.98

* No sampling

Table 4. Summary of the dynamic amplification of the stress in the strands at two typical locations.

SOFO sensor number	Centre-east position			Anchorage position		
	Stress in the strand 7km/h (MPa)	Stress in the strand 72km/h (MPa)	Dynamic amplification	Stress in the strand 7km/h (MPa)	Stress in the strand 72km/h (MPa)	Dynamic amplification
1	16.79	19.44	1.16	17.98	19.00	1.06
2	19.36	21.62	1.12	10.43	12.52	1.20
3	15.56	19.19	1.23	17.71	19.30	1.09
4	16.51	19.57	1.19	17.05	20.96	1.23
5	*	16.99		15.36	17.26	1.12
6	14.48	*		21.34	24.10	1.13
Mean value	16.54	19.36	1.17	16.64	18.86	1.14

* No sampling

5 CONCLUSION

The various measurements that were taken when the main cable of the Île-d'Orléans bridge was opened enabled us to successfully and precisely determine the state of the cable strands (corrosion and strength). The levels of stress under dead loads were then determined using laser interferometry. The vehicular live load level was confirmed using SOFO sensors. The quasi-static mean values that were calculated using a 3D finite element model were validated. However, not all of the strands in a given section were subjected to equal stresses. Our findings show differences in behaviour between the sections that were studied. Finally, dynamic amplification factors were calculated for each of the two sections.

6 ACKNOWLEDGEMENTS

We would like to thank Messrs Vandal, Rodrigue, Villeneuve, Rousseau, Godbout, Boulay and Ricard from the Ministère des transports du Québec for their valuable assistance on site, and Messrs Thivierge de Roctest and Inaudi from Smartec for helping us with the fibre optic data acquisition system.

REFERENCES

BREVET, P., OLIVIÉ, F., GUILBAUD, J. P. & RAHARINAIVO, A., (2004). « Microstructure et propriétés mécaniques des aciers pour câbles. Synthèse des travaux du LCPC (1970-2000). I. Plasticité et endommagement. », Bulletin *des laboratoires des Ponts et Chaussées*, mars-avril, pp. 35-48.

BREVET, P., RAHARINAIVO, A. & SIEGERT, D., (2004). « Microstructure et propriétés mécaniques des aciers pour câbles. Synthèse des travaux du LCPC (1970-2000). II. Ténacité, fissuration sous contrainte et fatigue. », *Bulletin des laboratoires des Ponts et Chaussées*, mai-août, pp. 75-92.

CRÉMONA, C. (2003). "Probabilistic approach for cable residual strength assessment.", *Engineering Structures*, 25, pp. 377-384.

CUNHA, A. & CAETANO, E., (1999). "Dynamic measurements on stay cables of cable-stayed bridges using an interferometry laser system." *Experimental Techniques*, May-June, pp. 38 43.

DEL GROSSO, A., TORRE, A., INAUDI, D., BRUNETTI, G. & PIETROGRANDE, A., (2005). "Monitoring System for a Cable-Stayed Bridge using static and dynamic Fiber Optic Sensors." 2nd International Conference on Structural Health Monitoring of Intelligent Infrastructure (SHMII-2005), Shenzhen, China, November 16-18.

ELACHACHI, S. M., BREYSSE, D., YOTTE, S. & CRÉMONA, C., (2005). « Analyse multi-échelle de la résistance du câble porteur d'un pont suspendu. Description de la corrosion et de ses effets par une approche probabiliste. », *Revue européenne de génie civil*, vol. 9, no 4, pp. 455 496.

GODART, B. & KRETZ, T., (2001). "Replacement of the suspension of the Aquitaine Bridge in Bordeaux." ASCE Structure Congress, Washington, May 21.

GAUTIER, Y., MORETTI, O. & CREMONA, C., (2005). "Universal Curves for a practical estimation of Cable Tension by Frequency Measurements.", International Conference on Experimental Vibration Analysis for Civil Engineering Structures (EVACES), Bordeaux, France, pp. 261-269.

GOURMELON, J.-P. (1986). « Ponts suspendus et ponts à haubans. », Fascicule 34 tiré de « Instruction technique pour la surveillance et l'entretien des ouvrages d'art. », LCPC SETRA.

GOURMELON, J.-P. (1997). « Pathologie des câbles de suspension. », Chapitre 12 tiré de « *Maintenance et réparation des ponts.* », Presses de l'École nationale des ponts et chaussées.

KRETZ, T., BREVET, P., CREMONA, C., GODART, B. & PAILLUSSEAU, P., (2006). « Haute surveillance et évaluation de l'aptitude au service du pont suspendu d'Aquitaine. », *Bulletin des laboratoires des Ponts et Chaussées*, mars, pp. 13-22.

MAHMOUD, K. (2006). "Evaluation of the remaining strength of bridge cables." 5th International Cable-Supported Bridge Operators' Conference, New York, August 28-29.

NCHRP 534 (2004). "Guidelines for Inspection and Strength Evaluation of Suspension Bridge Parallel Wire Cables." TRB's National Cooperative Highway Research Program (NCHRP).

PRIDHAM, B., STOYANOFF, S., DALLAIRE, P.E., TALBOT, M. & BRASSARD, A., (2006). "Toward more realistic predictions of long span bridge flutter.", International Conference on Bridge Engineering- Challenges in the 21st Century, Hong Kong, November 1-3.

ROBERT, J.-L. (1993). « Mesure de la tension des câbles par vibration.», Méthode d'essai LPC no 35, Laboratoire central des ponts et chaussées, France.

STAHL, F. L., & GAGNON, C. P., (1996). "*Cable corrosion in bridges and structures*.". ASCE Press, New York.

SIEGERT, D., DIENG, L., BREVET, P. & TOULEMONDE, F., (2005). "Parameter identification of a hanger or stay-cable model based on measured resonant frequencies." International Conference on Experimental Vibration Analysis for Civil Engineering Structures (EVACES), Bordeaux, France, pp. 469-476.

TALBOT, M. (2001). « Mesure de la tension dans les suspentes et les torons des câbles porteurs du pont de l'Île-d'Orléans par une méthode d'interférométrie laser. », 8e Colloque sur la progression de la recherche québécoise sur les ouvrages d'art, Université Laval, Québec, Canada, pp. 17-1 à 17-16.

TALBOT, M. (2002). « Méthodes expérimentales et numériques utilisées pour l'évaluation du pont suspendu de l'Île-d'Orléans. », 4e Conférence spécialisée en génie des structures de la Société canadienne de génie civil, Montréal, Québec, Canada.

TALBOT, M. & STOYANOFF, S., (2005). "Full-scale modal measurements of the I'Ile d'Orleans suspension bridge." International Conference on Experimental Vibration Analysis for Civil Engineering Structures (EVACES), Bordeaux, France.

TALBOT, M., HALCHINI, C. & SAVARD, M., (1993). "Load testing and numerical modeling of Quebec bridges." Proceedings of the IABSE colloquium on Remaining Structural Capacity, Copenhagen, pp. 283 290.

TALBOT, M. & LAFLAMME, J.-F. (2007). «Observations et mesures expérimentales lors de l'ouverture d'un câble porteur.», 14e Colloque sur la progression de la recherche québécoise sur les ouvrages d'art, Université Laval, Québec, Canada